

Topology of the nervous system of *Notommata copeus* (Rotifera: Monogononta) revealed with anti-FMRFamide, -SCPb, and -serotonin (5-HT) immunohistochemistry

Rick Hochberg^a

Department of Biological Sciences, University of Massachusetts, Lowell, Massachusetts 01854, USA

Abstract. The nervous system of the benthic freshwater rotifer, *Notommata copeus*, was examined using antibody probes, epifluorescence and confocal laser scanning microscopy, and digital imaging to highlight similarities with other monogonont rotifers. Immunoreactivity to anti-FMRFamide (Phe–Met–Arg–Phe–NH₂), -SCPb (small cardioactive peptide b), and -serotonin (5-HT, 5-hydroxytryptamine) was present in the central, peripheral, and stomatogastric nervous system. Specifically, anti-FMRFamide and -SCPb staining was abundant in perikarya and neurites of the cerebral ganglion, ventrolateral nerve cords, and mastax. In addition, a single loop-like neurite was present in between the nerve cords at the posterior end of the body. Serotonergic neurites were also abundant, and highlighted several cerebral pathways that included connections to the nerve cords and possibly the mastax. Novel neural pathways were also present in the posterior trunk region, where serotonergic neurites innervated the foot and lateral body wall. The results presented herein also highlight the utility of 3D visualization software to gain further insights into the organization and architecture of the rotifer cerebral ganglion.

Additional key words: rotifer, CLSM, cerebral ganglion

Rotifera is a morphologically diverse taxon of aquatic, bilaterally symmetrical micrometazoans typical of lotic and lentic environments. Historically characterized as simple metazoans (Remane 1929–1933; Hyman 1951), rotifers have recently been shown to possess complex anatomies as revealed in the structure of their trophi (Sørensen 2002) and the organization of their muscular systems (Hochberg & Litvaitis 2000; Kotikova et al. 2001, 2004; Sørensen et al. 2003; Santo et al. 2005; Sørensen 2005a,b). Phylogenetic diversity of Rotifera is also more complex than previously thought, with the inclusion of the parasitic Acanthocephala based on molecular sequence and ultrastructural data (reviewed in Funch et al. 2005), and the recent discovery of Micrognathozoa, a group comprising microscopic species with pharyngeal hard parts similar to rotiferan trophi (Funch et al. 2005). Our knowledge of genomic diversity has also increased substantially, especially regarding the bdelloid rotifers (Arkhipova & Meselson 2000; Welch & Meselson 2000). Indeed, as methods for probing these micrometazoans increase in complexity, our knowledge of their anatomy and evolution is bound to im-

prove and dramatically change our impressions about the apparent simplicity of their organization.

Within the past two decades, advances in microscopy and histological probes have provided incredible opportunities to study a variety of organ systems that are difficult to visualize using traditional methodologies. In particular, the muscular and nervous systems, historically described using light optics and histological stains, are now being revealed with remarkable clarity using fluorescent probes, novel antibodies, and high-resolution fluorescence microscopy. For example, the use of fluorescent phalloxin stains to label F-actin has provided new insights into the organization and function of the rotifer muscular system (Hochberg & Litvaitis 2000; Kotikova et al. 2001; Sørensen et al. 2003; Santo et al. 2005; Sørensen 2005a,b) and may eventually provide new characters for phylogenetic reconstruction (Sørensen 2005a). Similarly, histochemical studies of the rotifer nervous system have revealed unique neural topologies (Nogrady & Alai 1983; Raineri 1984; Keshmirian & Nogrady 1987, 1988; Kotikova 1995, 1997, 1998) and novelties in brain organization that may lead to a better understanding of rotifer phylogeny (Kotikova 1998). These early studies of nervous system organization relied almost exclusively on

^a E-mail: rick_hochberg@uml.edu

chemical reactions between fixatives and endogenous neurotransmitters to produce a histochemical fluorescence that was captured with standard epifluorescence microscopy. Nowadays, the availability of antibody probes for neurotransmitters and neural proteins, and the use of high-resolution optics with a computer interface, such as with confocal laser scanning microscopes, has the potential to dramatically increase our knowledge of the rotifer nervous system at both the structural and functional levels of organization (see Kotikova et al. 2005; Hochberg 2006).

The aim of the present investigation is to gain new insights into the structure of the nervous system in a common freshwater rotifer, *Notommata copeus* EHRENBERG 1834. Fluorescence microscopy and antibodies to three neurotransmitters, FMRFamide (Phe–Met–Arg–Phe–NH₂), SCPb (small cardioactive peptide b), and 5-hydroxytryptamine (5HT, serotonin), are combined with digital 3D imaging software to describe the topology of the nervous system. These patterns are then compared with the known distribution of neurons in other species of Monogononta in an attempt to discern their systematic value.

Methods

Collection

Specimens of *Notommata copeus* were collected with a 64- μ m plankton net from small lakes at the West Palm Beach Airport, FL, in February and March 2005. Rotifers were anesthetized in 1% MgCl₂ or 1 mmol L⁻¹ bupivacaine and photographed alive as whole mounts on glass slides, or subsequently processed in Hoyer's medium for clearing. Specimens were identified according to the taxonomic keys of Nogrady & Pourriot (1995) and Jersabek et al. (2003).

Immunohistochemistry

Thirty-seven rotifers were anesthetized and fixed in 4% paraformaldehyde in 0.1 mol L⁻¹ PBS for 24 h at 4°C. Despite anesthetization, many rotifers still contracted upon contact with the fixative. Specimens were next rinsed (4 \times) over the course of 24 h in 0.1 mol L⁻¹ PBS and then placed in an IT Signal Enhancer (Ingenta, Cambridge, MA) for 1 h to minimize non-specific staining. Thirty-two specimens were transferred to primary antibodies of anti-rabbit FMRFamide (dilution 1:500, $N = 12$; Abcam, Cambridge, MA), anti-rabbit serotonin (dilution 1:200, $N = 11$; Sigma-Aldrich, St. Louis, MO), or anti-mouse SCPb (dilution 1:100, $N = 9$; courtesy of Dr.

Scott Santagata) in 1.5 mL centrifuge tubes at 4°C on an orbital shaker for 48 h. All antibodies were diluted with PBT (0.1 mol L⁻¹ PBS plus 0.5% Triton X-100). Five specimens were used as controls and omitted from the primary antibodies. Specimens were then rinsed (3 \times) in 0.1 mol L⁻¹ PBS >24 h and transferred to appropriate secondary antibodies (PBT dilution 1:200): goat anti-rabbit Alexa-Fluor 546 (Sigma-Aldrich) and rat anti-mouse Alexa-Fluor 546 (Sigma-Aldrich). Specimens were stained in the dark at 4°C and on an orbital shaker for 24 h and then rinsed in 0.1 mol L⁻¹ PBT for 24 h. All specimens were subsequently stained in Alexa-Fluor 488 phalloidin for 1 h before mounting in Fluoromount G (Electron Microscopy Sciences, Hatfield, PA). Phalloidin staining was used to provide an anatomical framework for visualizing the nerves that might innervate the mastax.

Whole-mount specimens were examined on two microscopes: a Zeiss (Thornwood, NY) Axioimager equipped with epifluorescence, digital AxioCam MRm, and Zeiss software at the University of Massachusetts Lowell; and a Nikon (Melville, NY) Eclipse E800 compound microscope equipped with a Biorad (Hercules, CA) Radiance 2000 laser system (CLSM) at the Smithsonian Marine Station in Fort Pierce, FL. The specimens examined on the Zeiss microscope were kept refrigerated for 2 months before examination. The specimens examined on the CLSM were examined within 1 week of staining. Lasersharp (Hercules, CA) software was used to collect a series of 0.1- μ m optical sections with maximum intensity projection along the z -axis. Confocal images were imported into Confocal Assistant and made into TIF files. Additional digital files were imported into Volocity (Improvision) to render 3D images and create X – Y – Z rotations (TIF, AVI files). The rotatable AVI movies were necessary to trace the routes of neurons. No manipulations of the original images were made other than changes of color (false color or gray scale) or cropping. The program Carnoy V 2.0 (© 2001 Biovolution, Belgium) was used to make measurements of neurons in some digital images.

Results

Taxonomic identification

Specimens were identified by a combination of the following characters in live specimens (see Fig. 1): body length of 500–850 μ m, a thick mucilaginous sheet around the body, T-shaped auricles in swimming specimens, a long retrocerebral sac, a minute knob-like projection between the paired toes, a conical tail dorsal to the toes, paired long lateral setae, a

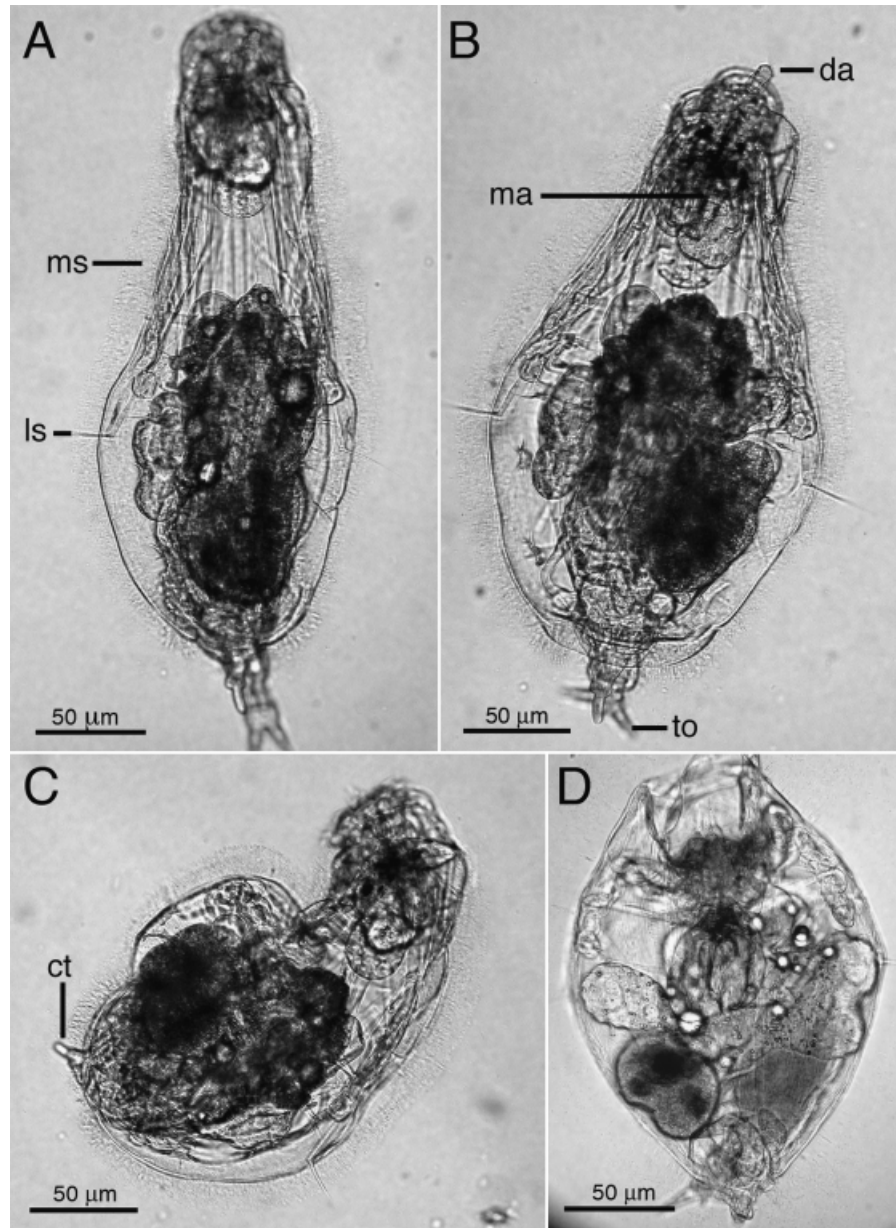


Fig. 1. A live specimen of *Notommata copeus* undergoing longitudinal contraction. **A.** Relaxed specimen. **B.** Slight longitudinal contraction initiated with a touch stimulus (microneedle). **C.** Near-complete longitudinal contraction following the touch stimulus. **D.** Complete contraction in the longitudinal plane. ct, conical tail; da, dorsal antenna; ls, lateral seta; ma, mastax; ms, mucilaginous sheath; to, toe.

long dorsal antenna that is constricted at the base, and bladder not observed. Fixed whole-mount specimens revealed the following characters of the trophus: slightly curved asymmetric manubria (50–65 µm), stout and long fulcrum (63–75 µm), and triangular rami. Microscopic details of the unci were difficult to visualize.

Live observation

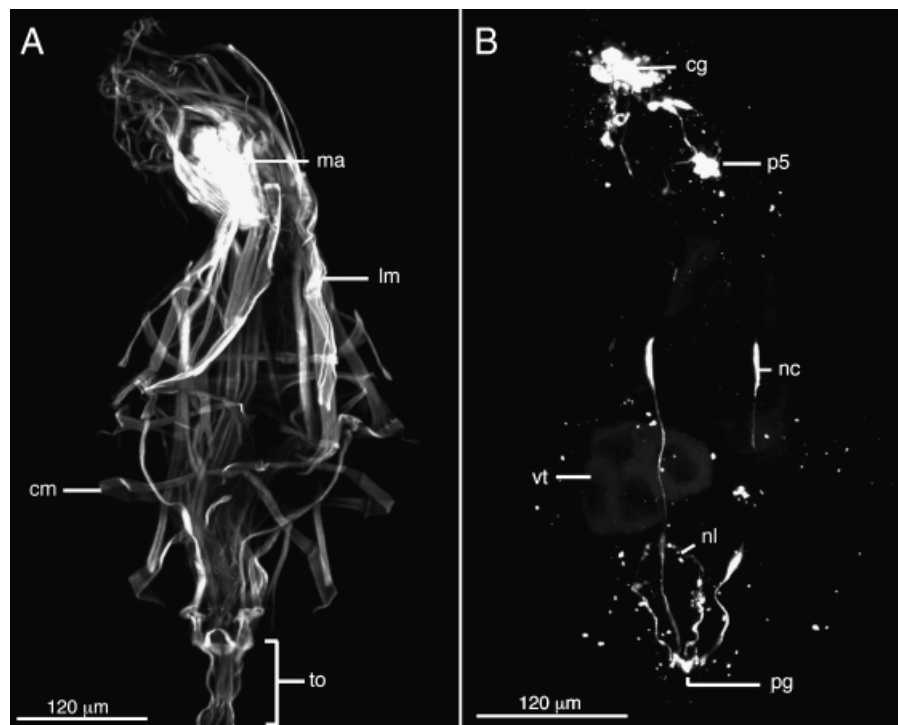
Specimens of *Notommata copeus* engaged in regular bouts of benthic creeping and ciliary gliding in a Petri dish. In creeping (foraging?) specimens, the animals moved slowly along the substratum in an ex-

tended shape, occasionally contracting into a spherical mass when encountering other animals (Fig. 1). Gliding rotifers were observed to extend their ciliated auricles and spiral slowly through the water column.

Anti-FMRamide and anti-SCPb immunoreactivity

FMRamide-like and -SCPb immunoreactivity was present in the central nervous system (cerebral ganglion, nerve cords) and the stomatogastric nervous system (mastax). Additional neurites were present in the posterior body region (Figs. 2–4). The distribution of immunoreactivity among specimens stained with a single antibody was similar, as was the

Fig. 2. Lateral views of a single, double-stained specimen (anti-SCPb and phalloidin) of *Notommata copeus*. **A.** Z-projection of the phalloidin-stained musculature in a whole animal. $0.1\ \mu\text{m} \times 200$ optical sections. **B.** Same specimen showing anti-SCPb immunoreactivity. $0.1\ \mu\text{m} \times 200$ optical sections. Note the lack of immunoreactivity in the anterior portion of the nerve cords. cg, cerebral ganglion; cm, circular muscle; lm, longitudinal muscle; ma, mastax musculature; nc, nerve cord; nl, neural loop; pg, pedal ganglion; p5, large single perikaryon of mastax; to, toe region; vt, vitellarium.



distribution of immunoreactivity between antibodies. Colocalization studies were not performed. Fluorescence was absent from control specimens.

Central nervous system. The cerebral ganglion measured $75\ \mu\text{m}$ wide \times $36\ \mu\text{m}$ long in a $750\ \mu\text{m}$ long, slightly contracted specimen (Fig. 3A). Variation in the total size of the cerebral ganglion among specimens was not measured. Individual perikarya were discernible and immunoreactivity was variable throughout the brain. In general, peripheral perikarya displayed lower immunoreactivity than central perikarya (Fig. 3A). More than 30 perikarya could be discerned, most of which were oval in shape and $\sim 5\text{--}8\ \mu\text{m}$ long \times $4\text{--}5\ \mu\text{m}$ wide. Few tractable neurites were evident within the cerebral ganglion, although a single commissure was present in many specimens (Fig. 3A, cc). Posteriorly, three connectives projected from the cerebral ganglion: one medial neurite (mn) and two lateral longitudinal neurites (ln). A commissure connected all three neurites $\sim 20\ \mu\text{m}$ below the brain (Figs. 3A, 4A, atc). A pair of small perikarya was present around the midline of this connection (Figs. 3A, 4A, mp). The lateral neurites continued posteriorly, where each terminated on a larger perikaryon (p2). A single neurite projected medially off each perikaryon toward neurons associated with the stomatogastric nervous system. A second neurite projected anterolaterally off each perikaryon (p2) and made contact with a second perikaryon (Fig. 3A, p3).

A pair of ventrolateral nerve cords (nc, ca. $1.5\text{--}2\ \mu\text{m}$ wide) was present in the trunk region (Figs. 2, 4A,B, nc). There was no discernible immunoreactivity in the nerve cords at their anterior end (about one-third body length), and so there was no obvious connection between the nerve cords and any connectives that exited the cerebral ganglion (Figs. 2B, 3A). Anteriorly, a single commissure joined the nerve cords just below the mastax (Fig. 4, tc). Posteriorly, the nerve cords followed the contour of the body and connected at the midline just above the jointed articulations of the toes. A ganglion was present at the midline (not shown). A pair of neurites, ca. $30\ \mu\text{m}$ long, projected laterally from where the nerve cords coalesced (Fig. 4A, pln). A pair of pedal perikarya was present in the first segmental region of the toes. Each perikaryon sent a short connective anteriorly toward the ganglion at the base of the nerve cords (Fig. 4A,B, pp). A loop-like neurite, ca. $71\ \mu\text{m}$ long and $37\ \mu\text{m}$ wide, projected from between the nerve cords at the body midline (Figs. 2B, 4A,B, nl). It was undetermined whether this loop encircled the intestine or portions of the reproductive system.

Stomatogastric nervous system. The mastax was innervated by ≥ 7 perikarya (Figs. 3, 4). The most anterior perikarya (p4) were a pair of bilateral cells connected to each other by a U-shaped commissure (ca. $10\ \mu\text{m}$ long); these perikarya were also contacted by neurites that extended from more lateral perikarya (Figs. 3A, 4A, p2). A second pair of perikarya (p3),

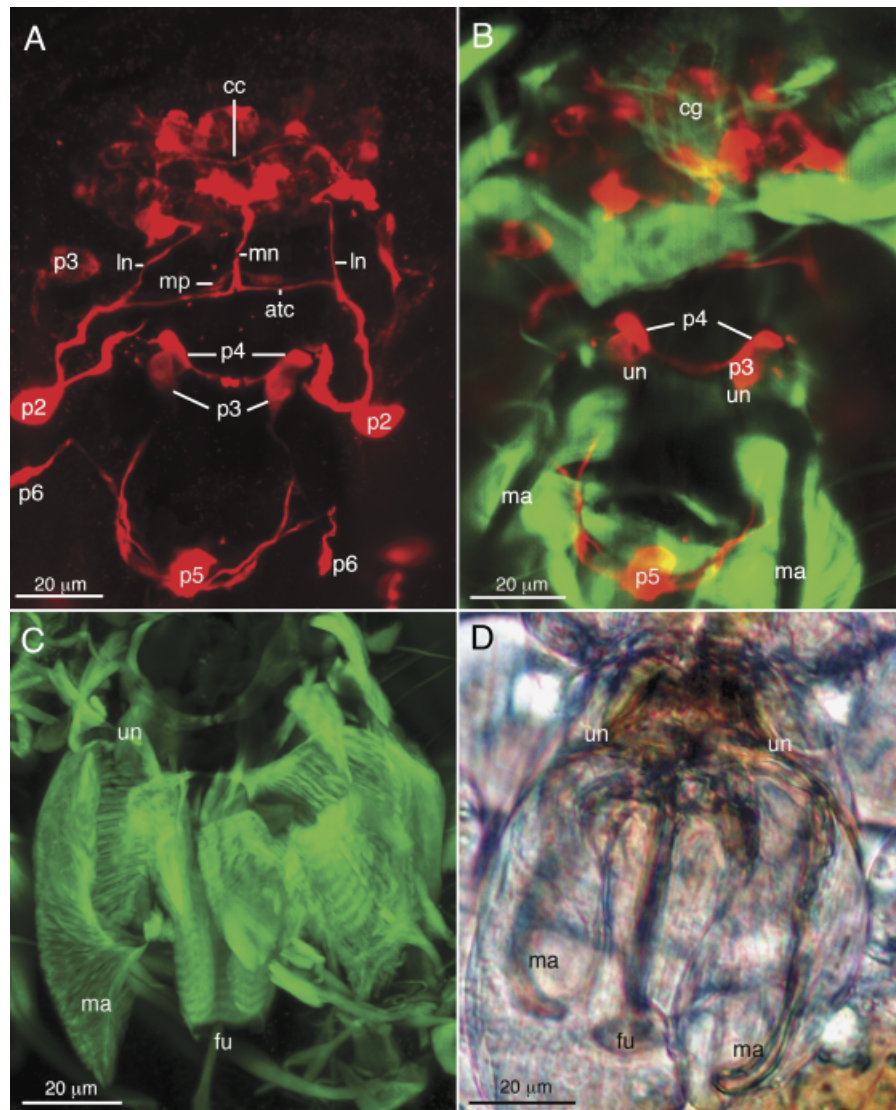


Fig. 3. Dorsal views of the anterior end of a double-stained specimen (anti-FMRamide and phalloidin) of *Notommata copeus*. **A.** Z-projection of anti-FMRamide immunoreactivity in the region of the cerebral ganglion and mastax. $0.1\mu\text{m} \times 181$ optical sections. **B.** Merge image of phalloidin staining and anti-FMRamide staining. $0.1\mu\text{m} \times 60$ optical sections. **C.** Epifluorescence image of mastax musculature. **D.** Light micrograph of mastax in a living specimen. atc, anterior transverse commissure; cc, cerebral commissure; cg, cerebral ganglion; fu, fulcrum or relative position of fulcrum; ln, lateral longitudinal neurite; ma, manubrium or relative position of manubrium; mn, medial neurite; mp, medial perikaryon; p2–p6, large perikarya of anterior trunk and mastax regions; un, uncus or relative position of the uncus.

positioned slightly ventral to the mastax unci (Figs. 3B, 4C, un), each sent a neurite (ca. $50\mu\text{m}$) toward the base of a large, individual perikaryon (p5, ca. $11 \times 7\mu\text{m}$) just ventral of the fulcrum. A second pair of eye-shaped perikarya (p6, ca. $4\text{--}5\mu\text{m}$) outside and lateral of the mastax appeared to contact the large, central perikaryon by way of a single long neurite (ca. $40\mu\text{m}$).

5-HT (serotonin) immunoreactivity

The general pattern of serotonin immunoreactivity was similar to that of anti-FMRamide and -SCPb immunoreactivity, with the strongest fluorescence signals present in the central nervous system (Fig. 5). Peripheral neurites and perikarya associated with the stomatogastric nervous system contained much weaker immunoreactivity.

Central nervous system. Numerous perikarya and neurites were present in the cerebral ganglion (Figs. 6, 7). The size of the brain in a single specimen (body length = $658\mu\text{m}$), determined by measuring the distance between the most peripheral perikarya, was $58\mu\text{m}$ wide \times $29\mu\text{m}$ long. Connections among perikarya were consistent among specimens regardless of the state of animal contraction. However, the meandering nature of the fibrous neurites made the determination of specific connections to sensory or motor devices very difficult, and many fibers that projected outside of the cerebral ganglion quickly lost their immunoreactivity.

Only five pairs of perikarya could be easily identified in the cerebral ganglion of different specimens. At the anterior end of the cerebral ganglion was a large pair of unipolar perikarya (lp, ca. $7\mu\text{m}$ wide \times $15\mu\text{m}$ long) that sat atop the brain (Figs. 6, 7). These

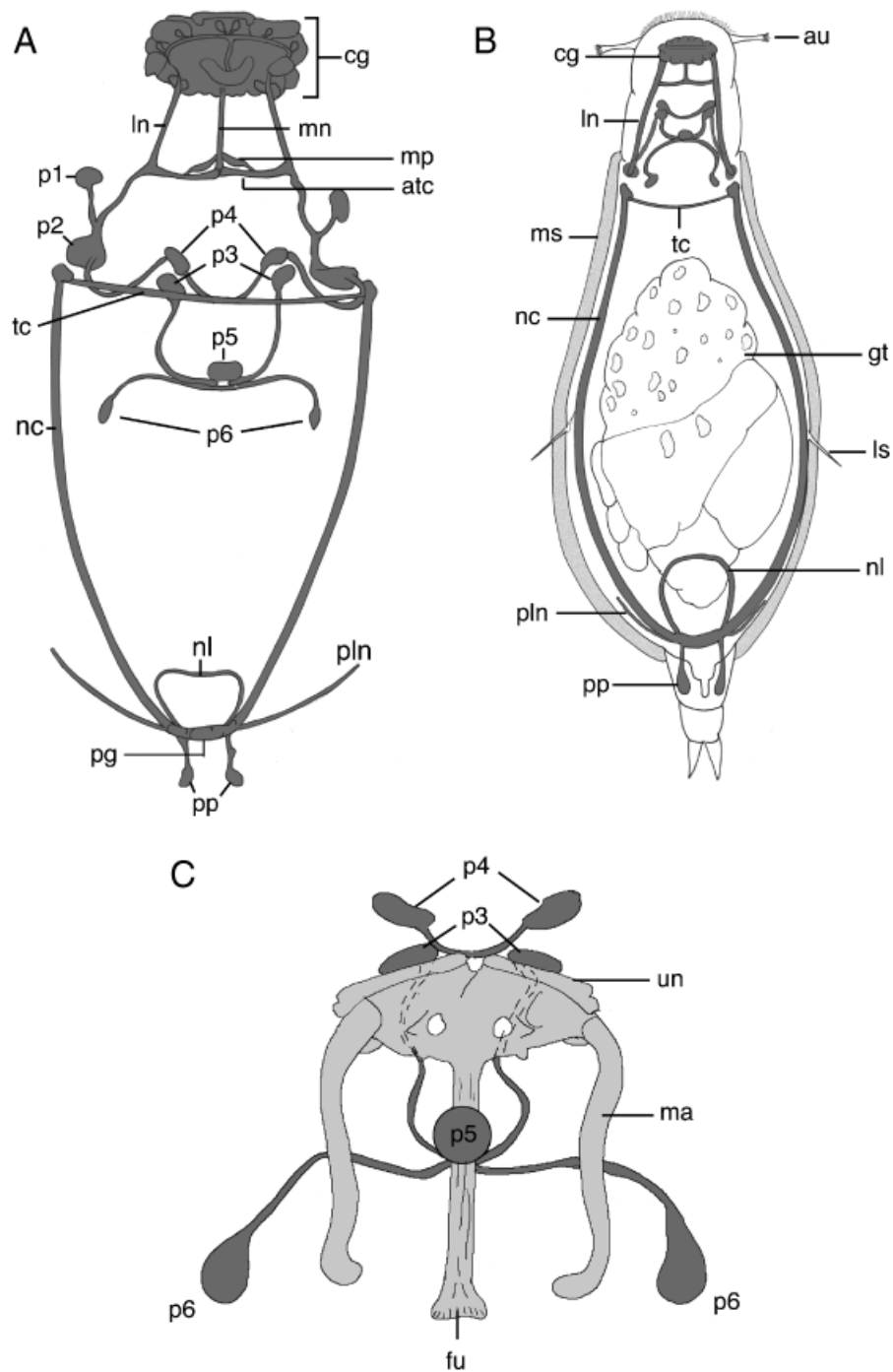


Fig. 4. Schematic illustrations of the nervous system of *Notommata copeus*. **A.** Organization of anti-FMRFamide immunoreactivity in the nervous system of a slightly contracted specimen. **B.** Schematic of anti-SCPb immunoreactivity in the nervous system of a relaxed specimen. **C.** Schematic of perikarya and neurites arranged around the mastax based on anti-FMRFamide immunoreactivity. atc, anterior transverse commissure; au, auricle; cg, cerebral ganglion; fu, fulcrum; gt, gut; ln, lateral longitudinal neurite; ls, lateral seta; ma, manubrium; mn, medial neurite; mp, medial perikaryon; ms, mucilaginous sheath; nc, nerve cord; nl, neural loop; pg, pedal ganglion; pln, posterolateral neurite; pp, pedal perikaryon; p1–p6, large perikarya of anterior trunk and mastax regions; tc, transverse commissure of the nerve cords; un, uncus.

cells appeared to partially encircle a pair of bipolar perikarya (mp) that sent neurites to the mastax. Slightly anterior and ventral to the large perikarya was the anterior commissure of the nerve cords (Figs. 6, 7, com). The commissure was $\sim 2\mu\text{m}$ in diameter and $16\mu\text{m}$ wide. A pair of eye-shaped perikarya (ep1) was positioned dorsal to the commissure, and a second pair was present posterior to the commissure (Fig. 7). The combination of the commissure and

the posterior cell bodies gave the appearance of an x-shaped structure (see Figs. 6, 7). Each small perikaryon sent a thin U-shaped neurite toward the ipsilateral nerve cord (Fig. 7). Closely associated with the end of this neurite was an eye-shaped perikaryon (ep2, ca. $3\mu\text{m}$ long) that sat atop the nerve cord and a much larger perikaryon (vp, ca. $8\text{--}10\mu\text{m}$ diameter) positioned below it. Several other cells were present in the cerebral ganglion, but in most cases their immuno-

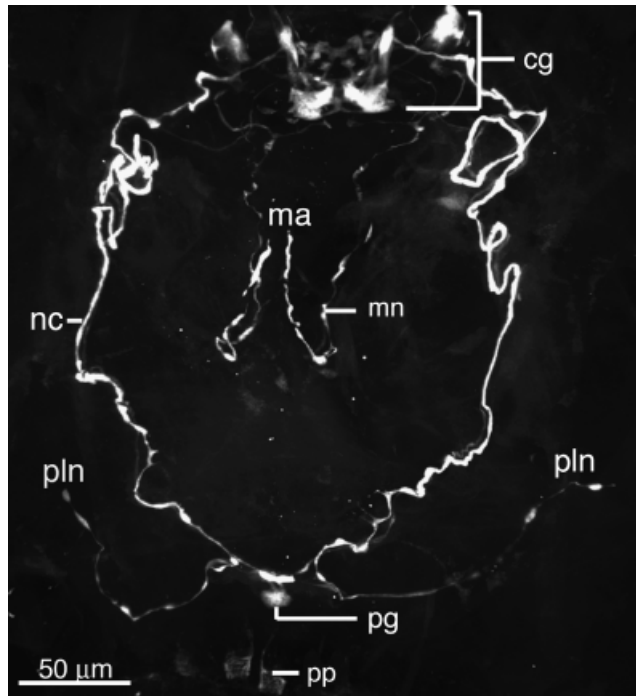


Fig. 5. Epifluorescence image of anti-serotonin immunoreactivity in a contracted specimen of *Notommata copeus*. cg, cerebral ganglion; ma, region of mastax; mn, neurite that extends from the cerebral ganglion to the mastax; nc, nerve cord; pg, pedal ganglion; pln, posterolateral neurite; pp, pedal perikaryon.

reactivity was too weak to make an accurate assessment of their size or connections. In addition, there were several immunoreactive neurites that formed meandering paths throughout the brain, but their convoluted nature was difficult to compare among specimens (Fig. 6).

The nerve cords displayed strong immunoreactivity along their entire length and, in contracted specimens, were often curled or kinked at the anterior end (Fig. 5). The nerve cords coalesced at the posterior end of the body; a small ganglion was present (Fig. 5, pg). Two posterior perikarya were connected to the commissure, each by a thin connective $\sim 25\text{--}30\ \mu\text{m}$ long (Fig. 5, pp). An additional pair of thin neurites extended $\sim 60\text{--}70\ \mu\text{m}$ from the posterior commissure to a site along the lateral body wall (Fig. 5, pln).

Stomatogastric nervous system. The mastax appeared to be innervated by a pair of long thin neurites that extended from the cerebral ganglion (Figs. 5, 6). Within the cerebral ganglion was a pair of bipolar, eye-shaped perikarya with long thin neurites that projected in anterior and posterior directions (mc, Figs. 5, 6). The posterior neurites exited the cerebral ganglion and could not be followed. The anterior neurites projected toward the front of the brain before curving posteroventrally for $65\text{--}80\ \mu\text{m}$. These

same fibers then curved again and projected anteriorly for $30\text{--}40\ \mu\text{m}$ toward the mastax. A direct association with the mastax could not be determined, but their termination was close to the base of the pharyngeal muscles.

Discussion

The nervous system of *Notommata copeus* revealed with antibody probes is comparable with other species examined in a similar manner (Kotikova et al. 2005; Hochberg 2006) and broadly analogous to specimens examined using earlier histochemical procedures (Raineri 1984; Keshmirian & Nogrady 1987, 1988; Kotikova 1995, 1997, 1998). Moreover, the gross anatomy of the central nervous system matches the general pattern present in Rotifera, with a dorsal cerebral ganglion showing clear bilateral symmetry of perikarya and neurites, and paired ventrolateral nerve cords connected by a transverse commissure. The stomatogastric nervous system is defined by perikarya and neurites closely associated with the mastax. In addition, peripheral perikarya and neurites are associated with the toes and posterior region of the trunk.

FMRFamide-like and serotonergic immunoreactivity in the central nervous system of *N. copeus* is similar to other monogononts, particularly *Platyias patulus*, *Euchlanis dilatata*, and *Asplanchna herricki*. In general, anti-FMRFamide staining reveals groups of perikarya clustered together in the cerebral ganglion but little in the way of obvious connectivity among them (see Kotikova et al. 2005). Some intracerebral wiring is evident in *N. copeus*, but without fully relaxed specimens, it remains difficult to determine the targets of the FMRFamidergic-like innervation. The same appears true of anti-SCPb staining, although colocalization studies were not performed, and it is speculative to suggest that the staining and targets of innervation were identical. Alternatively, anti-5HT staining reveals fewer perikarya in the cerebral ganglion—as observed in other taxa—but intracerebral pathways are much more pronounced, though still difficult to trace due to the overlapping nature of the neurites. In point of fact, the wiring of the cerebral ganglion in *N. copeus* is much more complex than has been revealed in earlier studies of other monogononts (Kotikova et al. 2005). Whether this complexity is due to increased connections in the cerebral ganglion, increased immunoreactivity, and/or a greater resolution with the microscopes and software remains unknown. However, one certainty in this study, according to the author, is that the use of 3D visualization software to create rotations of the

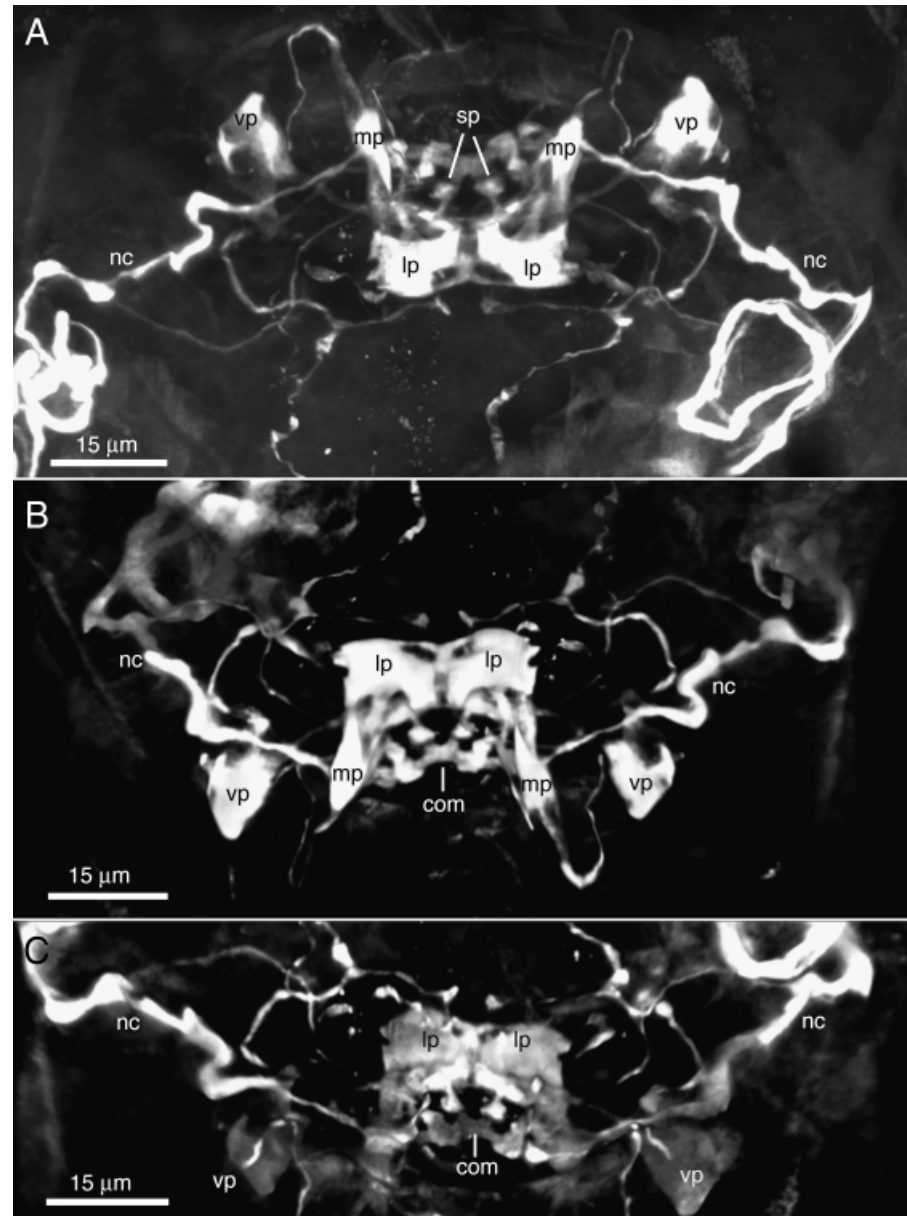


Fig. 6. Anti-serotonin immunoreactivity in the cerebral ganglion of *Notommata copeus*. **A.** Dorsal view of cerebral ganglion visualized using confocal microscopy. $0.05\ \mu\text{m} \times 272$ optical sections. **B.** Same image but digitally rotated to achieve an *en face* (anterior) view. **C.** Same image but digitally rotated to achieve a posterior view from between the nerve cords. See text for a detailed explanation of abbreviations. com, commissure; lp, large anterior perikaryon; mp, perikaryon that innervates the mastax region (compare with mn in Fig. 5); nc, nerve cord; sp, small perikaryon; vp, ventral perikaryon.

cerebral ganglion helped clarify many of the connections not easily visualized in a static (dorsal or ventral) view. Also, individual cells and their connections were easier to discern after digital movies of optical slices were produced, allowing for comparisons of wiring diagrams between specimens.

Furthermore, based on numerous 3D rotations of the cerebral ganglion, there does appear to be some significant regional specialization in the brain. For example, serotonergic and FMRamide-like cell bodies are clustered into discrete zones both within the brain and along its periphery. Unfortunately, without better visualization of their interconnections or sites of innervation, it remains difficult to homologize cerebral

cells in *N. copeus* with cells in other species (e.g., species examined by Kotikova et al. 2005). However, there are similarities in other regions of the central, stomatogastric, and peripheral nervous systems among species. For example, FMRamide-like immunoreactivity is present in the nerve cords, mastax ganglia, and neurites in the posterior body region of nearly all species examined to date. Curiously, a consistent feature in *N. copeus* was an almost complete lack of immunoreactivity in the region between the neurites that exited the brain (ln, the presumed nerve cords) and the nerve cords that appeared to originate *de novo* in the anterior trunk region (Fig. 2, nc). The lack of connection is not due to any anatomical gap in

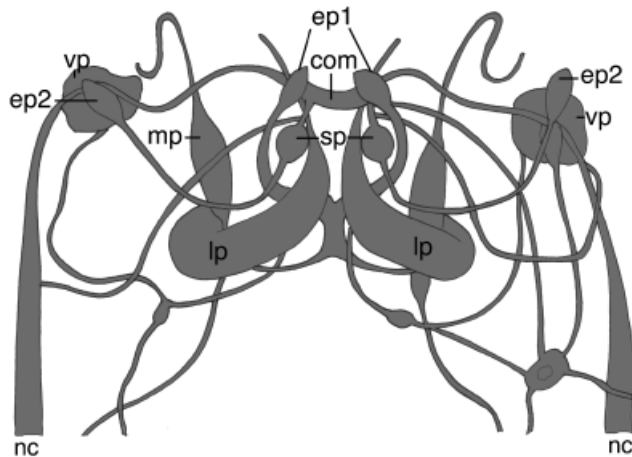


Fig. 7. Serotonergic wiring diagram of the cerebral ganglion (dorsal view) of *Notommata copeus*. Only those perikarya and neurites that could be easily identified in multiple specimens are labeled. See text for further explanation. com, commissure; ep1, eye-shaped perikaryon 1; ep2, eye-shaped perikaryon 2; lp, large anterior perikaryon; mp, perikaryon that innervates the mastax region (compare with mn in Fig. 5); nc, nerve cord; sp, small perikaryon; vp, ventral perikaryon.

the cords themselves. This is evidenced by the fact that 5HT immunoreactivity in the nerve cords is continuous along their entire length from the cerebral ganglion to the posterior body region. Kotikova et al. (2005) also demonstrated uninterrupted 5HT immunoreactivity in the nerve cords of three species, and found that serotonin and FMRFamide were not colocalized in the same nerve cord neurons. This suggests that the gap in immunoreactivity for *N. copeus* may be due to a localized absence of FMRFamide-containing neurons in that region (SCPb immunoreactivity is also absent).

The stomatogastric nervous system that innervates the mastax is also defined by a variety of neurons that possess immunoreactivity to all three neurotransmitters, with greatest immunoreactivity observed in FMRFamide and SCPb-containing perikarya (Fig. 3). Because of the degree of contraction of many specimens, the details about mastax innervation remain somewhat ambiguous, and caution is important in interpreting the results. The mastax receives innervation from ≥ 7 FMRFamide and SCPb-containing perikarya. A single perikaryon is positioned in the center of the mastax close to the fulcrum; it is in close proximity to a pair of posterior neurites outside of the mastax and a pair of neurites close to the unci. Additional perikarya and neurites were present just anterior of the mastax, including an unusual geometric configuration of perikarya and neurites posterior of the brain (Figs. 3A, 4). Despite their proximity to the mastax, it is hypothesized that only some of the

anterior perikarya actually innervate the mastax directly. Others may innervate as yet undetermined organs in the region of the mastax (e.g., somatic muscles, retrocerebral apparatus). Innervation by serotonergic fibers is even more ambiguous and distinctly different from that of FMRFamide and SCPb. A single pair of neurites projects from the brain and into the posterior trunk region, where they curve anteriorly and appear to innervate a zone around the mastax. The precise target of these neurites is difficult to determine, but they terminate close to the base of the pharynx. These results add to the growing knowledge about mastax innervation, which appears to be highly variable based on information from Kotikova et al. (2005). For example, both FMRFamide and serotonergic neurons innervate the mastax in *E. dilatata* and *A. herricki*, whereas only FMRFamide-like immunoreactivity is present in *P. patulus*. Moreover, the patterns of neural innervation, and the number of perikarya, are different among species. In the future, a larger systematic effort with greater species sampling will be necessary to make sense of these results.

Peripheral innervation of the trunk region of *N. copeus*, particularly the foot and toes, is comparable with that observed in *P. patulus* and *E. dilatata*. In all three species, FMRFamide neurites form a pathway between the nerve cords and foot and/or toes, but only in *P. patulus* and *E. dilatata* are three pairs of perikarya present (see Kotikova et al. 2005), as opposed to a single pair in *N. copeus*. Additionally, a pair of long, thin neurites project out from the base of the nerve cord commissure in *N. copeus* and into the lateral body region. The targets of innervation are unknown, as the direction of the neurites differed among specimens in different states of contraction. Most unusual, however, was the presence of a neural loop at the base of the nerve cords. The neural loop did not appear to terminate on any organ system, but may in fact form a sensory ring around the intestine or reproductive system.

To date, the nervous system of 23 species and 18 genera of Rotifera have been examined using various whole-mount procedures. Twenty of these species are monogononts, and 19 species belong to the subclade Ploima. Ploimate rotifers are highly diverse in anatomy and lifestyle, but as can be seen in the current analysis, possess several similarities in nervous system staining and topology that may be of use in future studies of rotifer phylogeny, evolution, and behavior. As noted by Kotikova et al. (2005), many species possess FMRFamide-like immunoreactivity in neurons that occupy similar positions with respect to the neuropile, and therefore may be homologous. It is

also noteworthy that in all rotifers examined using antibody-specific probes, the number of FMRFamide-containing neurons generally outnumbers the serotonergic neurons. This is especially evident in the cerebral ganglion of *A. herricki*, and in the lack of serotonin immunoreactivity in the foot, and to some degree the mastax and corona of *P. patulus* and *E. dilatata* (Kotikova et al. 2005). Similar patterns were evident in *N. copeus*, but await further details because not all perikarya could be easily identified or enumerated in the cerebral ganglion, nor conclusively linked with the meandering neurites that made up a large proportion of the immunoreactivity. Future studies would be wise to evaluate antibody-specific neural patterns against a phylogeny of the Monogononta such as that of Sørensen (2002) to determine evolutionary trends in innervation or homologies among rotifers sharing similar lifestyles (e.g., planktonic vs. benthic).

Acknowledgments. I thank the editor and two anonymous reviewers for their constructive criticism of this manuscript. I also thank the staff of the Smithsonian Marine Station for the use of their facilities and their support. This research received financial support from the University of Massachusetts Lowell and from the Sumner Gerard Foundation through a postdoctoral fellowship to the Smithsonian Marine Station at Fort Pierce, FL. This is Smithsonian Marine Station at Fort Pierce contribution # 707.

References

- Arkhipova I & Meselson M 2000. Transposable elements in sexual and ancient asexual taxa. *Proc. Natl. Acad. Sci. USA* 97: 14473–14477.
- Funch P, Sørensen MV, & Obst M 2005. On the phylogenetic position of Rotifera—have we come any further? *Hydrobiologia* 546: 11–28.
- Hochberg R 2006. On the serotonergic nervous system of two planktonic rotifers, *Conochilus coenobasis* and *C. dossuarius* (Monogononta, Flosculariacea, Conochilidae). *Zool. Anz.* 245: 53–62.
- Hochberg R & Litvaitis MK 2000. Functional morphology of the muscles in *Philodina* sp. (Rotifera: Bdelloidea). *Hydrobiologia* 432: 57–64.
- Hyman LR 1951. *The Invertebrates: Acanthocephala, Aschelminthes, and Entoprocta. The Pseudocoelomate Bilateria*, Vol. III. McGraw Hill, New York.
- Jersabek CD, Segers H, & Dingmann BJ 2003. *The Frank J. Meyers Rotifer Collection at The Academy of Natural Sciences: The whole collection in digital images. (CD-ROM)*. The Academy of Natural Sciences of Philadelphia, Special Publication 20.
- Keshmirian J & Nogrady T 1987. Histochemical labelling of catecholaminergic structures in rotifer (Aschelminthes) in whole mount animals. *Histochemistry* 87: 351–357.
- 1988. Histochemical labelling of catecholaminergic structures in rotifers (Aschelminthes). II. Males of *Brachionus plicatilis* and structures from sectioned females. *Histochemistry* 89: 189–192.
- Kotikova EA 1995. Localization and neuroanatomy of catecholaminergic neurons in some rotifer species. *Hydrobiologia* 313/314: 123–127.
- 1997. Localization of catecholamines in the nervous system of *Transversiramida*. *Dokl. Russ. Acad. Sci.* 353: 841–843.
- 1998. Catecholaminergic neurons in the brain of rotifers. *Hydrobiologia* 387/388: 135–140.
- Kotikova EA, Raikova OI, Flyatchinskaya LP, Reuter M, & Gustafsson MKS 2001. Rotifer muscles as revealed by phalloidin-TRITC staining and confocal scanning laser microscopy. *Acta Zool.* 82: 1–9.
- Kotikova EA, Raikova OI, Reuter M, & Gustafsson MKS 2004. Musculature of an illoricate rotifer *Asplanchnopus multiceps* as revealed by phalloidin fluorescence and confocal microscopy. *Tissue Cell.* 36: 189–195.
- 2005. Rotifer nervous system visualized by FMRFamide and 5-HT immunohistochemistry and confocal laser scanning microscopy. *Hydrobiologia* 546: 239–248.
- Nogrady T & Alai M 1983. Cholinergic neurotransmission in rotifers. *Hydrobiologia* 104: 149–153.
- Nogrady T, Pourriot R, & Segers H 1995. The Notommataidae and The Scardiidae. In: *Rotifera 3, Guides to the Identification of the Microinvertebrates of the Continental Waters of the World*. 8. Rotifera. Dumont H & Nogrady T, eds. SPB Academic, The Hague, The Netherlands. 248 pp.
- Raineri M 1984. Histochemical investigations of Rotifera Bdelloidea. I. Localization of cholinesterase activity. *Histochem. J.* 16: 601–616.
- Remane A 1929–1933. *Rotatoria*. In: *Klassen und Ordnung des Tierreichs*, Vol. 4, Sect II. Book 1, Part 3. Bronn HG, ed., Akademische Verlagsgesellschaft, Leipzig, Germany. 596 pp.
- Santo N, Fontaneto D, Fascio U, Melone G, & Caprioli M 2005. External morphology and muscle arrangement of *Brachionus urceolaris*, *Floscularia ringens*, *Hexarthra mira* and *Notommata glyphura* (Rotifera, Monogononta). *Hydrobiologia* 546: 223–229.
- Sørensen MV 2002. On the evolution and morphology of the rotiferan trophi, with a cladistic analysis of Rotifera. *J. Zool. Syst. Evol. Res.* 40: 129–154.
- 2005a. Musculature in three species of *Proales* (Monogononta, Rotifera) stained with phalloidin-linked fluorescent dye. *Zoomorphology* 124: 47–55.
- 2005b. Musculature of *Testudinella patina* (Rotifera: Flosculariacea), revealed with CLSM. *Hydrobiologia* 546: 231–238.
- Sørensen MV, Funch P, Hooge M, & Tyler S 2003. Musculature of *Notholca acuminata* (Rotifera: Ploima: Brachionidae) revealed by confocal scanning laser microscopy. *Invert. Biol.* 122: 223–230.
- Welch DM & Meselson M 2000. Evidence for the evolution of bdelloid rotifers without sexual reproduction or genetic exchange. *Science* 288: 1211–1215.